Towards Direct Numerical Simulation of ternary systems in contact with a wall using PLIC-based contact line modeling

J. Wurst*[1], K. Schulte[1]
[1] Institute for Aerospace Thermodynamics, University of Stuttgart, Germany
*Corresponding author: jonathan.wurst@itlr.uni-stuttgart.de

Introduction

Drop wall interactions involving not only one liquid but another immiscible liquid phase offer great potential in advanced applications such as cell printing or oil remediation. Being able to simulate such processes helps in understanding and designing them. We therefore develop a simulation framework to simulate a ternary system in contact with a wall. Starting from the framework of Potyka and Schulte [4], our in-house multiphase flow solver *Free Surface 3D* [2] is extended to accurately simulate the associated contact line dynamics at the wall. The contact angle boundary condition proposed by Sussman [6] is extended for the second liquid phase and applies a local averaged contact angle to distinguish between the contact lines. A short introduction to the theory on compound sessile drops is then followed by several static tests of the code.

Material and methods

The in-house code *Free Surface 3D* (FS3D) [2] is further developed for a ternary system in contact with a wall. It is based on the Finite Volume method and applies the Volume-of-Fluid method (VoF) [3] together with the piecewise linear interface calculation (PLIC) [5] to distinguish between the phases. For the reconstruction of the interface, the method proposed by Potyka and Schulte [4] is employed. Where an interface is in contact with a solid boundary, the surface tension force has to be adjusted according to the wettability. This is usually achieved by imposing a specific contact angle. For this purpose, we extend the method of Sussman [6] to be able to simulate three immiscible phases in contact with a wall.

Contact Angle Boundary Condition - At a wall boundary, there is no full stencil available for the calculation of the surface tension force. The idea of Sussman's method [6] is to provide this missing information by extending the interface into the ghost cells. This approach is independent of the surface tension model and can be applied to immersed boundaries as well. With the wall normal $\mathbf{n}_{wall}$ and the interface normal $\mathbf{n}_f$, an artificial velocity $\mathbf{u}_{ext}$ is constructed by

$$\boldsymbol{u}_{ext} = \frac{\boldsymbol{n}_{wall} + \cot(\theta)\boldsymbol{n}_2}{|\boldsymbol{n}_{wall} + \cot(\theta)\boldsymbol{n}_2|}, \tag{1}$$

$$\boldsymbol{n}_2 = -\frac{\boldsymbol{n}_1 \times \boldsymbol{n}_{wall}}{|\boldsymbol{n}_1 \times \boldsymbol{n}_{wall}|}, \tag{2}$$

$$\boldsymbol{n}_1 = -\frac{\boldsymbol{n}_f \times \boldsymbol{n}_{wall}}{|\boldsymbol{n}_f \times \boldsymbol{n}_{wall}|}, \tag{3}$$

where $\mathbf{n}_1$ and $\mathbf{n}_2$ are auxiliary vectors in the wall plane and point tangential and orthogonal to the contact line, respectively. By executing several steps of the advection scheme with an artificial time step of $\Delta t = 0.5\Delta z|\boldsymbol{u}_{ext}|^{-1}$, the ghost cells are filled with liquid and provide information about the interface.

With a second immiscible liquid phase, two more types of contact lines can form with distinct contact angles θ_{ij} between the phases i and j. A sketch of such a situation is displayed in Figure 1. Throughout this paper, we specify the continuous gaseous phase as phase 3 and the liquid phases as 1 and 2. Adopting the idea of Zhang et al. [7], the local contact angle $\theta_i(\boldsymbol{x})$ at coordinates $\boldsymbol{x}$ of phase i is determined based on the phase fractions f_j and f_k via

$$\theta_i(\boldsymbol{x}) = \frac{f_j(\boldsymbol{x})}{f_j(\boldsymbol{x}) + f_k(\boldsymbol{x})}\theta_{ij} + \frac{f_k(\boldsymbol{x})}{f_j(\boldsymbol{x}) + f_k(\boldsymbol{x})}\theta_{ik}. \tag{4}$$

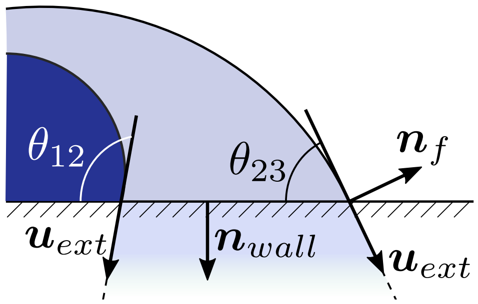

Figure 1. Sketch of Sussman's method. The extension velocity u_{ext} is constructed to transport the liquid according to the contact angle into the ghost cells.

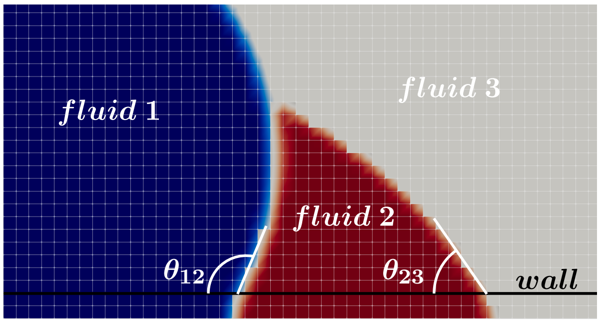

Figure 2. An exemplary VoF distribution after applying Sussman's method. The ghost cells inside the wall boundary contain the information of the extended interfaces.

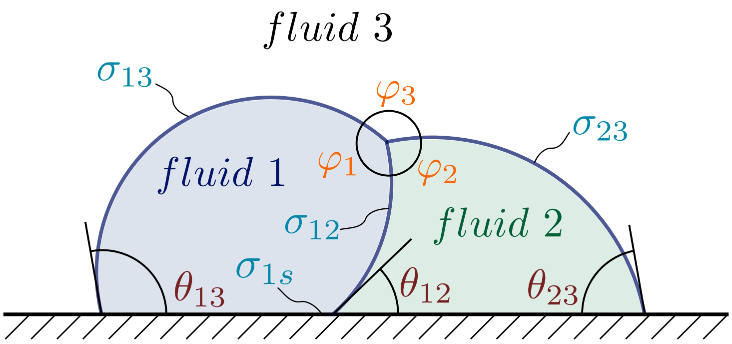

Figure 3. Janus drop configuration with all relevant properties like interfacial tensions σ_{ij}, contact angles θ_{ij}, and interfacial angles φ_i.

This contact angle is then used for the velocity construction in equation 1. In a first step, this procedure is only applied to fluid 1 while neglecting fluid 2 during the advection. Subsequently, the same is carried out for fluid 2. For the final result, the VoF distributions in the ghost cells of both fluids are superimposed. An exemplary VoF distribution is depicted in Figure 2.

Sessile Compound Droplet

Two immiscible liquids with a common interface and in contact with a wall can exhibit four different configurations. The most generic one is the Janus configuration, depicted in Figure 3. Two droplets of immiscible liquids are side by side and in touch with each other and the solid boundary. In total, three distinct contact lines and contact angles where three phases meet are present including the solid phase. Additionally, there are two points where all contact lines meet and hence all four phases exist, cf. Figure 5. The region where all three fluid phases meet is called the triple line and the angles between the three interfaces are the interfacial angles. Each phase has its own properties and characteristics towards other phases. So there are three interfacial tensions σ_{ij}, three solid-fluid interfacial tensions σ_{is}, three contact angles θ_{ij}, and three interfacial angles φ_i. The contact angles as well as interfacial angles obey the conditions

$$\theta_{ij} + \theta_{ji} = \pi, \tag{5}$$

$$\varphi_1 + \varphi_2 + \varphi_3 = 2\pi. \tag{6}$$

For each contact line, Young's equation can be formulated as

$$\sigma_{ij}\cos(\theta_{ij}) = \sigma_{js} - \sigma_{is}. \tag{7}$$

Furthermore, combining equation (7) for all contact angles, the unknown liquid-liquid contact angle can be determined with

$$\theta_{12} = \arccos\left(\frac{\sigma_{13}\cos(\theta_{13}) - \sigma_{23}\cos(\theta_{23})}{\sigma_{12}}\right), \tag{8}$$

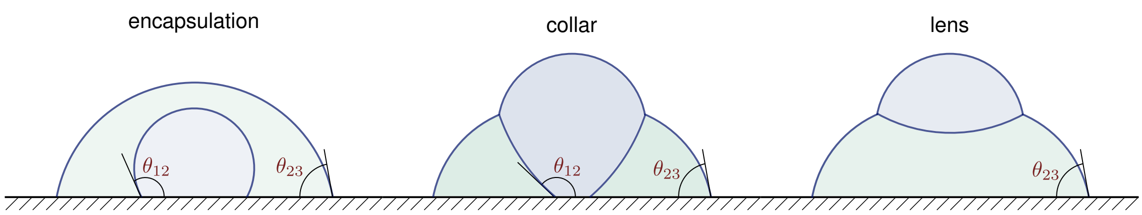

Figure 4. Sketches of the encapsulation, collar, and lens configurations with illustrated contact angles.

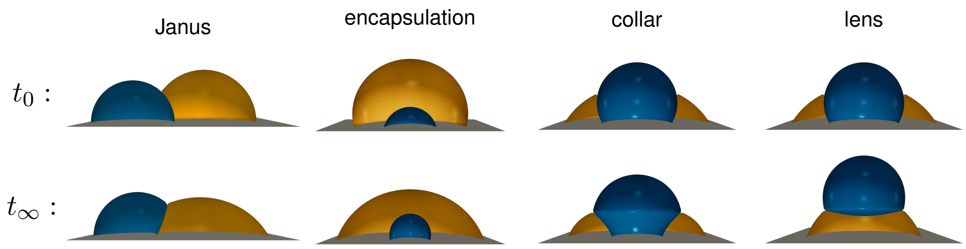

Figure 5. Simulation snapshots of the initial (t_0) and final (t_∞) states for all types of configurations.

as usually the liquid-gas contact angles as well as interfacial tensions can be looked up and in contrast the liquid-liquid contact angle is often unknown or cumbersome to obtain. Other configurations are the encapsulation, collar, and lens configuration, shown in Figure 4. A requirement for the triple line is the inequality

$$\sigma_{ij} < \sigma_{ik} + \sigma_{jk} \tag{9}$$

for all combinations. Otherwise, the liquid with the lower surface tension would cover the other liquid phase to form the encapsulation configuration, so that the surface energy is minimized.

Results and Discussion

The implementation is tested by reproducing all four static configurations of a sessile compound drop. Two immiscible drops are initialized as sections of spheres on a solid substrate in a configuration close to equilibrium. During the simulation, the drops should evolve towards the equilibrium with the correct contact angle. All fluid-fluid interfacial tensions are chosen as $\sigma_{ij} = 30\,\mathrm{mN\,m^{-1}}$ such that all configurations are stable. Solid-fluid interfacial tensions do not need to be specified explicitly but are fixed implicitly by assigning the contact angles. Moreover, the liquid-gas contact angles are set to $\theta_{13} = 90^\circ, \theta_{23} = 70^\circ$ which yields a liquid-liquid contact angle of $\theta_{12} = 110^\circ$. Figure 5 displays snapshots of the initial (t_0) and final (t_∞) state of four different simulations. All types of configurations are reproduced by the simulation and the droplets seem to adopt the correct contact angles. Interestingly, the initial setup for the collar and lens shapes is the same. Only the dynamic viscosity differs by a factor of 10 as $\mu_{collar} = 10\mu_{lens}$. This demonstrates that there is not always one unique stable solution and the dynamics can have an impact on the final state.

Conclusion

The solver FS3D was extended for simulations of wetting phenomena of a ternary system in contact with a wall. The implementation was tested to reproduce four different types of configurations that a sessile compound drop can exhibit. We therefore conclude that the presented framework is able to predict wetting phenomena of a ternary system. In future work, the simulation of dynamic contact lines will be pursued further to enable the simulation of compound droplet impacts with multiple contact lines.

Acknowledgment

We kindly acknowledge funding by the Deutsche Forschungsgemeinschaft (DFG) under Project-ID 270852890 – GRK 2160/2 and under Germany's Excellence Strategy – EXC 2075 – 390740016.

Nomenclature

f	phase fraction [-]	Δz	grid spacing [m]
$\boldsymbol{n}$	normal vector [-]	θ	contact angle [°]
$\boldsymbol{u}_{ext}$	extension velocity [m/s]	μ	dynamic viscosity [Pa s]
$\boldsymbol{x}$	coordinates [m]	σ	surface tension [N/m]
Δt	time step [s]	φ	interfacial angle [°]

References

[1] R. G. Cox. The dynamics of the spreading of liquids on a solid surface. part 1. viscous flow. *Journal of Fluid Mechanics*, 168(1):169, 1986.
[2] K. Eisenschmidt, M. Ertl, H. Gomaa, C. Kieffer-Roth, C. Meister, P. Rauschenberger, M. Reitzle, K. Schlottke, and B. Weigand. Direct numerical simulations for multiphase flows: An overview of the multiphase code FS3D. *Journal of Applied Mathematics and Computation*, 272(2):508–517, 2016.
[3] C. W. Hirt and B. D. Nichols. Volume of fluid (VOF) method for the dynamics of free boundaries. *Journal of Computational Physics*, 39(1):201–225, Jan. 1981.
[4] J. Potyka and K. Schulte. A volume of fluid method for three dimensional direct numerical simulations of immiscible droplet collisions. *International Journal of Multiphase Flow*, 170:104654, 2024.
[5] W. J. Rider and D. B. Kothe. Reconstructing volume tracking. *Journal of Computational Physics*, 141(2):112–152, Apr. 1998.
[6] M. Sussman. *An adaptive mesh algorithm for free surface flows in general geometries*. Chapman and Hall/CRC Boca Raton, FL, USA, 2001.
[7] C.-Y. Zhang, H. Ding, P. Gao, and Y.-L. Wu. Diffuse interface simulation of ternary fluids in contact with solid. *Journal of Computational Physics*, 309:37–51, 2016.